Distributed Tactile Display with Dual Array Design

Yerkebulan Massalim, Damien Faux, Vincent Hayward

Distributed Tactile Display with Dual Array Design

Yerkebulan Massalim, Damien Faux, and Vincent Hayward, *Life Fellow, IEEE*

Abstract—It is well-accepted that designing and manufacturing distributed tactile displays is hard owing to difficulties associated with packing many strong actuators in a small space. We explored a new design for such displays by reducing the number of independently actuated degrees of freedom while preserving the ability to decorrelate the signals applied to small regions of the fingertip skin inside the contact area. The device comprised two independently actuated tactile arrays so the degree of correlation of the waveforms stimulating those small regions could be globally controlled. We show that for periodic signals, the degree of correlation between the displacement of the two arrays was equivalent to setting the phase relationship between the displacements or the arrays or the mix of common and differential modes motions. We found that anti-correlating the displacements of the arrays significantly increased the subjective perceived intensity for the same displacement. We discussed the factors that could explain this finding.

Index Terms—Tactile displays, Haptics Interfaces, Tactile signals

1 Introduction

Since the introduction of the pioneering Optacon device in the mid-sixties [1], designers of distributed tactile displays faced stringent engineering tradeoffs owing to the desire to pack many actuated surfaces in a small space. The designers of the Optacon focused on a single function: mapping binary black-and-white images onto the equivalent tactile patterns on the fingertip [2], [3]. To this end, an array of 24×6 contact surfaces were vibrated at resonance ($\approx$ 250 Hz) by cantilevered bi-morph piezoelectric actuators. At rest, the surfaces were recessed. When activated, they collided with the skin, yielding highly localised sensations because of transient high frequency components. These sensations provide the sharp foreground/background contrast to identify pixellated binary tactile images on the fingertip.

Another notable design employed a similar strategy but with "the intention [$\cdots$] not to reproduce the topology of 'real' surfaces — rather, [$\cdots$] to reproduce an appropriate excitation pattern over the various populations of mechanoreceptors in the skin." [4]. The display was tested by asking observers to identify the direction of motion of lines across the array, and optimal stimulation parameters could be obtained.

Y. Massalim, D. Faux, and V. Hayward are with Actronika SAS, 75017, Paris, France. Y. Massalim is also with Laboratoire des Systèmes Perceptifs, Département d'Études Cognitives, École Normale Supérieure, PSL Université, CNRS, Paris, France. V. Hayward is also with Institut des Systèmes Intelligents et de Robotique, Sorbonne Université, 75005, Paris, France. Email: yerkebulan.massalim@actronika.com.

The tradeoffs between density, number, strength, bandwidth, compactness, complexity, and reliability have been variously addressed by others. Pneumatic actuation is attractive because of its ability to pack a large amount of power in a small space, *viz.* 10 $\mathrm{W/cm^2}$ [5]. The motion bandwidth, however, did not exceed 5 Hz for the latter device. For practical reasons, many designers focused on electrodynamic actuation. The use of commercial servomotors, for example, enabled the bandwidth of motion to be pushed to 25 Hz [6].

Another example was a device employing an 8×8 array of carefully engineered micro-coils [7]. The development of electrodynamically actuated, distributed tactile displays, however, is generally hampered by highly unfavourable scaling laws ($1/L^3$ to $1/L^4$) [8] that limit the number and the density of independent actuators, *e.g.* [9], [10], [11]. Many other devices, which cannot be exhaustively surveyed here for brevity, have been described and experimented with. A recent example of the technical challenges for such displays is described in [12].

A tactile device termed laterotactile leveraging a contact mechanic effect [13] displaces the contact surfaces of an array laterally [14]. This type of device can create vivid sensations of edges or textures [15], and multiple studies successfully used it [16], [17], [18] *inter alia*. Owing to structural limitations, however, the motion bandwidth was limited to 200 Hz.

Here, we abandoned the aim of generating arbitrary spatiotemporal patterns on the skin in favor of greater freedom in the temporal specification of stimulus production. We surmised that our somatosensory system is not in a position to independently process each *local* piece of information from the mechanoreceptors when scanning textured surfaces. Instead, the hypothesis was that *global* properties encoded in the relationships between these pieces of information, that is, phase information between the stimulations of small skin regions, had behavioural importance. A related concept was previously described by Asamura and al. [19], who explored the perceptual effects of phase relationships between localised stimuli on glabrous skin.

To test this hypothesis, we conjectured that a display featuring a small number of degrees of freedom but capable of specifying phase information would be sufficient to impact measures such as the perceived subjective equality of intensity when the phase was varied. To this end, we constructed a minimalist device featuring a dense array

of contacting surfaces and divided these surfaces into sets of interleaved contact surfaces, each controlled independently. We then asked volunteers to determine the Perceived Subjective Equivalence of Intensity (PSEI) between pairs of stimuli for different values of phase relationships.

We describe the device in Section 2. The stimuli and the experimental testing procedure are introduced in Section 3. Finally, the experiment results are presented and discussed in Sections 4 and 5.

2 Device

Uniformly distributed pins, arranged in a quincunx configuration, were grouped into interleaved arrays (red and blue) represented in Fig. 1a–c. The two arrays were independently actuated. The pins of the bottom and top plates had a height of 4 mm and 0.5 mm, respectively, so they terminated in the same plane. Each array comprised a 10×13 matrix of pins, each of 1.5 mm diameter with a rounded top. The top plate had through holes 2.0 mm in diameter that allowed the pins from the top plate to interleave without contact with the pins of the bottom plate.

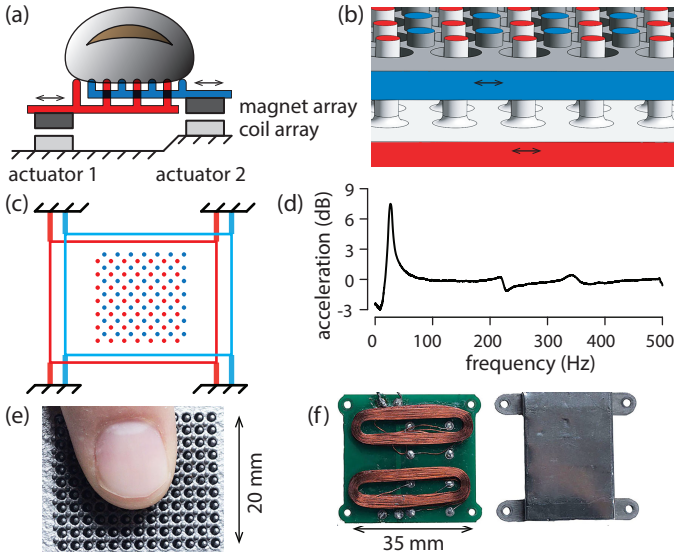

Fig. 1. Tactile Display Device. (a) Schematic arrangement with two independently actuated plates. (b) Top plate (blue) superposed to bottom plate (red). The apices of the pins terminated in the same plane. (c) Each plate was independently suspended. (d) Acceleration response. (e) Active surface. (f) Components of modular actuator.

The plates and pins were made of solid aluminium and manufactured using a Direct Metal Laser Sintering technique. Each array was independently actuated. The pin-bearing plates were mounted on 150×150×5 mm plexiglass frames, and small attachments were 3D-printed. Each plate was kinematically guided by a four-flexure suspension, see Fig.1c. The hardened aluminium flexures were 10×8×0.1 mm in size. The actuators were of a modular type with two close subassemblies. In the first subassembly, a Halbach magnet array interacted with an array of flat coils in a second subassembly [20]. Current passing through coils generates a Laplace force which generates the translational movement of the plates.

Because the actuators were quite powerful, we set the mass of the frames to be sufficiently high (200 g) to lower the natural frequency of the mass-spring oscillator down to about 30 Hz, thereby providing wide motion bandwidth. Large masses also had the advantage of providing the moving parts with high impedance, eliminating concerns related to modifying the system response when loaded by fingertips. This way, the current in the coils was mapped directly to motion acceleration. The response was typical of a damped mass-spring system. Inverse filtering flattened the system response such that the system bandwidth was 50–500 Hz ±2 dB, see Fig. 1d. A Graphical User Interface slider widget allowed participants to adjust the stimulation intensity on a scale from zero to three.

The acceleration response shown in Fig. 1d was measured using an accelerometer with ±20 G range, 10 kHz bandwidth (8778A500 Kistler, Winterthur, Switzerland). The electromechanical assembly was hooked up to a data acquisition card (NI USB-6366 DAQ, National Instruments, Austin, TX, USA), along with amplifiers (TS250, Accel Instruments, Gladbach, Germany) to drive the actuators. The sampling frequency was 30 kHz.

3 Methods

Waveforms: When in-phase and identical waveforms drove the arrays, the pins replicated the movement of a rigid body with a surface covered with closely packed protrusions. When the waveforms had a phase difference, the protrusions also generated local tractions on the skin. In other words, any pair of motions could be represented by a common mode motion corresponding to vibrating solid and a differential mode motion reflecting the simplified case of a finger sliding on a rough surface. Sliding a finger on such a surface generates uncorrelated movements of small regions of skin since it is unlikely that all contacts would be in the same state at the same time [21]. With our device, the degree of correlation between the two motions could be adjusted from the relative proportion of the two modes of motion.

To quantify this degree of correlation, consider the zero-delay normalised cross-correlation measure, $\mathrm{NCC}(s_1, s_2)$, between two sinusoidal waveforms $s_1(t)$ and $s_2(t)$ of angular frequency, ω, period, T, and phase difference ϕ. It can be written [22],

$$\begin{aligned}\mathrm{NCC}(s_1, s_2) &= \frac{\int_0^T s_1 s_2 \mathrm{d}t}{\sqrt{\int_0^T s_1^2 \mathrm{d}t \int_0^T s_2^2 \mathrm{d}t}}, \\ &= \frac{\int_0^T (\sin(\omega t - \phi/2)\sin(\omega t + \phi/2))\mathrm{d}t}{\sqrt{\int_0^T \sin(\omega t - \phi/2)^2 \mathrm{d}t \int_0^T \sin(\omega t + \phi/2)^2 \mathrm{d}t}}.\end{aligned}$$

Noting that $\sin(x)\sin(y) = \frac{1}{2}[\cos(x-y) - \cos(x+y)]$ and $\sin(x)^2 = \frac{1}{2}[1 - \cos(2x)]$, $x, y \in \mathbb{R}$, the expression becomes,

$$\mathrm{NCC}(s_1, s_2) = \frac{\frac{1}{2}\int_0^T [\cos(\phi) - \cos(2\omega t + \phi)]\mathrm{d}t}{\sqrt{\frac{1}{4}\int_0^T (1 - \cos(2\omega t - \phi))\mathrm{d}t \int_0^T (1 - \cos(2\omega t + \phi))\mathrm{d}t}}.$$

Since $\int_0^T \cos(2\omega t, -\phi) = 0$, and $\int_0^T \cos(2\omega t + \phi) = 0$, we can write,

$$\mathrm{NCC}(s_1, s_2) = \frac{T\cos(\phi)}{2}\frac{2}{T} = \cos(\phi).$$

We now identify the relation between the phase difference, ϕ, and the mix of common and differential modes of motion, $s_{\text{com}} = \frac{1}{2}(s_1 + s_2)$ and $s_{\text{diff}} = \frac{1}{2}(s_2 - s_1)$. To see that, decompose s_1 and s_2 into,

$$\begin{aligned} s_1 &= \cos(\phi/2)\sin(\omega t) - \sin(\phi/2)\cos(\omega t)\,, \\ s_2 &= \cos(\phi/2)\sin(\omega t) + \sin(\phi/2)\cos(\omega t)\,, \quad \text{thus,} \\ s_{\text{com}} &= \tfrac{1}{2}(s_1 + s_2) = \cos(\phi/2)\sin(\omega t)\,, \\ s_{\text{diff}} &= \tfrac{1}{2}(s_2 - s_1) = \sin(\phi/2)\cos(\omega t)\,. \end{aligned}$$

These expressions show that tuning ϕ sets the weights of common and differential modes. When the phase difference was zero, the motions of the two arrays were identical, that is, fully correlated. The motions were anti-correlated by setting the phase to π, resulting in the pure differential mode. Intermediary values provided a mix of differential and common modes of motion.

Stimuli: The hypothesis outlined in Section 1 was tested by determining of PSEIs between sinusoidal and complex waveforms when the phase was varied. The degrees of common and differential modes were adjusted by the phase difference between the motions of the two arrays.

To examine sensitivity to frequency, the tests were performed with sinusoidal waveforms of 60 Hz and 120 Hz. We also performed the tests with broadband, complex signals. To this end, complex waveforms were synthesised by first-order, low-pass filtering of white noise, leading to a $1/f$ noise signal. This waveform is of particular interest since tactual vibrations generated by a finger sliding on smooth and corrugated surfaces exhibit similar properties [21].

Phase differences were 0, $\pi/2$, and π corresponding to correlated, decorrelated, and anti-correlated stimuli. In random signals, phases are also random, *i.e.*, devoid of information. As a result, there is no direct manner to control the correlation between random $1/f$ signals without modifying the waveforms. We, therefore, restricted the phase differences to 0 and π. The five stimuli, illustrated in Fig. 2, resulted in ten meaningful pairs of stimuli. Pairs of identical stimuli served as a control baseline to ensure that the results were not biased.

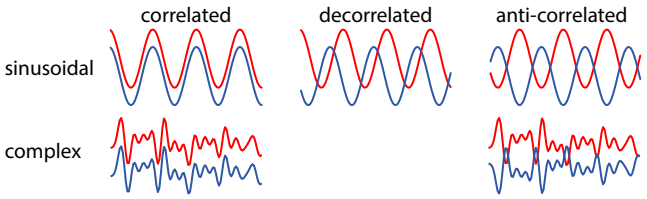

Fig. 2. Illustration of the test waveforms.

Procedure: Ten healthy, right-handed participants (seven males and three females, age range 20–31) volunteered their time for the experiment and provided written informed consent. The participants rested their dominant hand's index and middle fingers on the active surface. The motion of the active surface was along the ulnar-radial direction. They heard white noise through a headset to mask the faint noise emitted by the device. We adopted the method of adjustments to estimate the PSEIs. The use of this method is favourable when one is interested in the determination of absolute and differential thresholds because it is fast, simple, and minimises confounds due to boredom, distraction, adaptation, and drift in decision criterion [23], [24].

Since there were three types of stimuli for sinusoidal waveforms, nine combinations (3×3) of stimulus pairs ensued. The combinations led to four testing conditions: 'decorrelated v anti-correlated,' 'correlated v decorrelated,' and 'correlated v anti-correlated.' Stimuli in a pair could be identical, and the corresponding condition was labeled as 'identical pairs.' For complex signals, conditions were 'identical pairs' and 'correlated v anti-correlated.'

The experiment comprised two blocks, A and B, and adopted an AB-BA experimental plan to account for order effects. Five participants carried out the experiment in the AB order, and another five in the BA reversed order. In block A, the participants were presented with randomised pairs of sinusoidal stimuli with identical frequencies at each trial. There was a one-second interval between stimuli presentations. Participants matched the stimuli's perceived intensity by adjusting the magnitude of second stimulus. Block A comprised forty trials. The same procedure was employed in block B, but the stimuli were complex waveforms. Block B comprised twenty trials.

Participants could repeat the stimuli presentations whenever they felt it necessary. The participants initially required two or three repetitions to achieve a satisfactory perceived equivalence of intensities. Once they had internalised the mapping from cursor position to intensity, they typically achieved perceived equivalence of intensities in a single adjustment. The experiments took ten to fifteen minutes for each participant to complete.

4 Results & Analysis

Figure 3 collects the overall results.

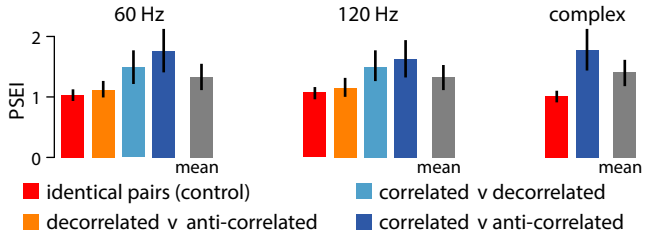

Fig. 3. Results. PSEI per conditions of stimulus pairs. Error bars: Standard deviation from the mean.

For the decorrelated v anti-correlated condition, the mean value was close to one for the 60 Hz and 120 Hz stimuli. Participants did not feel much difference between decorrelated and anti-correlated stimuli. For the correlated v decorrelated condition, however, we observed a significant bias in intensity toward the decorrelated stimulus with PSEI values of 1.47 and 1.48 at 60 Hz and 120 Hz, respectively. An even stronger trend was observed for the correlated v anti-correlated condition with PSEI values of 1.74 and 1.61 for the 60 Hz and 120 Hz, respectively.

For the complex waveforms, we obtained a PSEI value of 1.78 for correlated v anti-correlated pair. This bias meant that the perceived intensity provided by the differential mode

was almost twice stronger than the perceived intensity provided by the common motion mode.

We applied Welch's t-test to evaluate the distributions' differences among the various conditions [25]. Although the distributions did not meet the normality criterion as per the Anderson-Darling test [26], Welch's t-test is considered for most distributions to be sufficiently robust to deviations from normality to assess differences reliably. Table 1 summarises the results.

TABLE 1
Welch's test results and thresholds for 99% confidence level.

stimulus	condition	DoF	t-statistics	threshold
60 Hz	correlated/decorrelated	58	5.5	2.40
60 Hz	correlated/anti-correlated	55	7.0	2.41
120 Hz	correlated/decorrelated	59	5.4	2.40
120 Hz	correlated/anti-correlated	40	5.3	2.42
complex	correlated/anti-correlated	138	11.3	2.36

5 Discussion

The identical pairs condition, in all cases, see Fig. 3, led to PSEIs that were very close to one. It confirmed that estimates of perceived intensity were unbiased.

5.1 Peripheral Factors

The observed biases in perceived intensity could be related to mechanical effects since the contact mechanics problem corresponding to the common mode motion was very different from that corresponding to the differential mode motion. In the first instance, the entire gross contact area was entrained by uniform traction, causing subsurface strain that resembled the strain induced in a finger in contact with a vibrating object. In the second instance, the differential mode motion created a dynamic contact mechanics problem akin to the case of a finger sliding on a rough surface, minus the net component. Thus, tactile mechanics may have influenced the perceived intensity for the same displacement, as further discussed in the next subsection.

The spectral characteristics of the signals across the different conditions, including correlated and anti-correlated complex signals, were different because dynamic contact mechanics and mechano-transduction processes are strongly nonlinear and thus modify the spectra for a given excitation. The observed biases could thus be due to factors related to the frequency selectivity of mechanoreceptor populations. However, the mechanoreceptor populations classified according to their adaptation rates, exhibit a near absence of frequency selectivity beyond 4 Hz when excited at supra-threshold levels, see Fig 4. The influence of mechanoreceptor frequency specificity on our results is, therefore dubious. What is more likely is that different mechanoreceptor populations are tuned to detect different categories of transient micro-mechanical events, as first suggested in [19].

5.2 Perceptual Factors

The reader may have noticed that for sinusoidal waveforms the uniform progression of the perceived intensity as a function of the proportion of differential mode motion in the mix, or equivalently, to the degree of correlation between the motion of the two arrays, see Fig. 3. This observation is summarised in Table 2. What is the most significant is the large increase in PSEI in the complex waveform case. This point is further discussed in the next subsection.

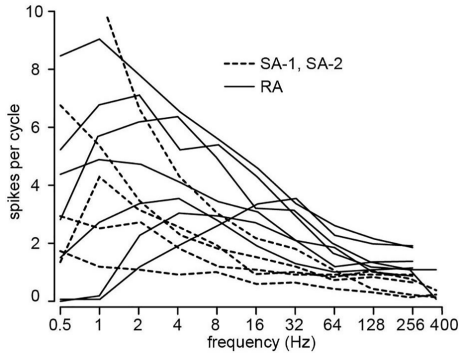

Fig. 4. Near absence frequency selectivity. Montage obtained by superposition of Fig. 2C and Fig. 4C of [27]. SA stands for slowly adapting, RA for rapidly adapting. Reproduced by permission from Elsevier.

TABLE 2
PSEI gains in % for each mix of motion modes or amount of correlation across waveforms and conditions (colour coding as in Fig. 3).

waveform	ϕ	s_{com}	s_{diff}	correlation	conditions
sinusoidal	0	1.0	0.0	+1.0	
	$\pi/2$	0.7	0.7	0.0	
	π	0.0	1.0	-1.0	
complex	π	0.0	1.0	-1.0	
relative gains					12% 48% 67% 76%

5.3 Cognitive Factors

Why could anti-correlated complex waveforms lead to a larger increase in perceived intensity than sinusoidal ones? It is appealing to invoke an explanation related to "top-down" models of perception, where the emergence of conscious sensations result from predictions made by the brain based on long-term exposure to certain sensory inputs that match short-term peripheral inputs. Such models relate percepts to categories of objective causes for sensory inputs.

These computational models, termed predictive coding models [28], stem from earlier cognitive models called 'analysis by synthesis models [29]. These models describe perception as a minimisation process of the prediction error between short-term peripheral inputs and signals from models learned over the long term. Such models have met with considerable success in the visual domain [30], [31], [32] and could be applied here to the tactile domain since complex tactile inputs are frequent in everyday life and throughout development, whereas sinusoidal waveforms are confined to occasional exposure to rotating machinery.

6 Conclusion and Future Work

The dual-array tactile display used for the experiments could be extended to configurations enabling more significant amounts of decorrelation between small regions

within the gross contact area of a fingertip. For example, the two-array system could be extended without significant technical obstacles to a three-array tactile display system enabling increased decorrelation options. The present system displaced the arrays along one single degree of freedom. The actuation system we have employed would readily support array displacements with two degrees of freedom. The two arrays would then each provide two degrees-of-freedoms and thus even greater decorrelation options. These options are the object of current developments.

Finally, several recent works have observed that the current level of realism elicited by presently available surface tactile displays is poor [33], [34], [35]. We have informally observed, even with the limited capabilities of the simplified system described here, a net increase in the realism of synthetic textures recreated from pre-recorded signals. The prospect of increasing the realism of synthetic tactual textures through decorrelation is also the subject of on-going investigations.

7 Acknowledgments

The research was supported by the project INTUITIVE, a MSCA-ITN funded by the EU Horizon 2020 under grant agreement No 861166. It was also supported by an ANR-17-EURE-0017 FrontCog grant. The authors wish to thank Henrik Jörntell of Lund University for insightful discussions.

References

[1] J. G. Linvill and J. C. Bliss, "A direct translation reading aid for the blind," Proceedings of the IEEE, vol. 54, no. 1, pp. 40–51, 1966.
[2] J. C. Bliss, M. H. Katcher, C. H. Rogers, and R. P. Shepard, "Optical-to-tactile image conversion for the blind," IEEE Transactions on Man-Machine Systems, vol. 11, no. 1, pp. 58–65, 1970.
[3] "https://en.wikipedia.org/wiki/optacon," Wikipedia, 07 2021.
[4] I. R. Summers and C. M. Chanter, "A broadband tactile array on the fingertip," The Journal of the Acoustical Society of America, vol. 112, no. 5, pp. 2118–2126, 2002.
[5] G. Moy, C. Wagner, and R. S. Fearing, "A compliant tactile display for teletaction," in IEEE International Conference on Robotics and Automation, vol. 4. IEEE, 2000, pp. 3409–3415.
[6] C. R. Wagner, S. J. Lederman, and R. D. Howe, "A tactile shape display using RC servomotors," in Proceedings of the Symposium on Haptic Interfaces For Virtual Environment And Teleoperator Systems, 2002, pp. 354–356.
[7] M. Benali-Khoudja, M. Hafez, and A. Kheddar, "Vital: An electromagnetic integrated tactile display," Displays, vol. 28, no. 3, pp. 133–144, 2007.
[8] O. Cugat, J. Delamare, and G. Reyne, "Magnetic micro-actuators and systems (MAGMAS)," IEEE Transactions on Magnetics, vol. 39, no. 6, pp. 3607–3612, 2003.
[9] J. Streque, A. Talbi, P. Pernod, and V. Preobrazhensky, "New magnetic microactuator design based on PDMS elastomer and MEMS technologies for tactile display," IEEE Transactions on Haptics, vol. 3, no. 2, pp. 88–97, 2010.
[10] S. Gallo, C. Son, H. J. Lee, H. Bleuler, and I.-J. Cho, "A flexible multimodal tactile display for delivering shape and material information," Sensors and Actuators A: Physical, vol. 236, pp. 180–189, 2015.
[11] J. J. Zárate and H. Shea, "Using pot-s to enable stable and scalable electromagnetic tactile displays," IEEE Transactions on Haptics, vol. 10, no. 1, pp. 106–112, 2016.
[12] R. V. Grigorii, J. E. Colgate, and R. L. Klatzky, "The spatial profile of skin indentation shapes tactile perception across stimulus frequencies," Scientific Reports, vol. 12, no. 1, pp. 1–11, 2022.
[13] Q. Wang and V. Hayward, "Tactile synthesis and perceptual inverse problems seen from the view point of contact mechanics," ACM Transactions on Applied Perception, vol. 5, no. 2, pp. 1–19, 2008.
[14] ——, "Biomechanically optimized distributed tactile transducer based on lateral skin deformation," The International Journal of Robotics Research, vol. 29, no. 4, pp. 323–335, 2010.
[15] V. Levesque and V. Hayward, "Tactile graphics rendering using three laterotactile drawing primitives," in Proceedings of the 16th Symposium on Haptic Interfaces For Virtual Environment And Teleoperator Systems, 2008, pp. 429–436.
[16] H. Jörntell, F. Bengtsson, P. Geborek, A. Spanne, A. V. Terekhov, and V. Hayward, "Segregation of tactile input features in neurons of the cuneate nucleus," Neuron, vol. 83, no. 6, pp. 1444–1452, 2014.
[17] L. Dupin, V. Hayward, and M. Wexler, "Direct coupling of haptic signals between hands," Proceedings of the National Academy of Sciences, vol. 112, no. 2, pp. 619–624, 2015.
[18] A. Moscatelli, V. Hayward, M. Wexler, and M. O. Ernst, "Illusory tactile motion perception: An analog of the visual filehne illusion," Scientific Reports, vol. 5, p. 14584, 2015.
[19] N. Asamura, N. Tomori, and H. Shinoda, "A tactile feeling display based on selective stimulation to skin receptors," in Proceedings. IEEE 1998 Virtual Reality Annual International Symposium. IEEE, 1998, pp. 36–42.
[20] V. Hayward, P. Comot, and R. Pijewski, "Vibrotactile actuator," US Patent 11,289,988, 2022.
[21] M. Wiertlewski, C. Hudin, and V. Hayward, "On the 1/f noise and non-integer harmonic decay of the interaction of a finger sliding on flat and sinusoidal surfaces," in Proceedings of World Haptics Conference, 2011, pp. 25–30.
[22] J. Martin and J. L. Crowley, "Comparison of correlation techniques," in Intelligent Autonomous Systems, 1995, pp. 86–93.
[23] W. H. Ehrenstein and A. Ehrenstein, "Psychophysical methods," in Modern Techniques in Neuroscience Research. Springer, 1999, pp. 1211–1241.
[24] C. C. Wier, W. Jesteadt, and D. M. Green, "A comparison of method-of-adjustment and forced-choice procedures in frequency discrimination," Perception & Psychophysics, vol. 19, no. 1, pp. 75–79, 1976.
[25] B. Derrick, D. Toher, and P. White, "Why Welch's test is type i error robust," The Quantitative Methods in Psychology, vol. 12, no. 1, 2016.
[26] N. M. Razali, Y. B. Wah et al., "Power comparisons of shapiro-wilk, kolmogorov-smirnov, lilliefors and anderson-darling tests," Journal of Statistical Modeling and Analytics, vol. 2, no. 1, pp. 21–33, 2011.
[27] R. S. Johansson, U. Landström, and R. Lundström, "Responses of mechanoreceptive afferent units in the glabrous skin of the human hand to sinusoidal skin displacements," Brain Research, vol. 244, no. 1, pp. 17–25, 1982.
[28] K. Friston, "Functional integration and inference in the brain," Progress in Neurobiology, vol. 68, pp. 113–143, 2002.
[29] U. Neisser, Cognitive Psychology. New York: Appleton-Century-Crofts, 1967.
[30] D. H. Ballard, G. E. Hinton, and T. J. Sejnowski, "Parallel visual computation," Nature, vol. 306, pp. 21–26, 1983.
[31] D. Mumford, "On the computational architecture of the neocortex II. The role of cortico-cortical loops," Biological Cybernetics, vol. 66, pp. 241–251, 1992.
[32] M. Kawato, H. Hayakawa, and T. Inui, "A forward-inverse optics model of reciprocal connections between visual cortical areas," Network: Computation in Neural Systems, vol. 4, no. 4, pp. 415–422, 1993.
[33] M. Wiertlewski, J. Lozada, and V. Hayward, "The spatial spectrum of tangential skin displacement can encode tactual texture," IEEE Transactions on Robotics, vol. 27, no. 3, pp. 461–472, 2011.
[34] S. Bochereau, S. Sinclair, and V. Hayward, "Perceptual constancy in the reproduction of virtual tactile textures with surface displays," ACM Transactions on Applied Perception (TAP), vol. 15, no. 2, pp. 1–12, 2018.
[35] R. V. Grigorii, R. L. Klatzky, and J. E. Colgate, "Data-driven playback of natural tactile texture via broadband friction modulation." IEEE Transactions on Haptics, 2021.